SDC-91-00052

SDC
SOLENOIDAL DETECTOR NOTES

FIBER-TILE OPTICAL STUDIES AT ARGONNE

D.G. Underwood, D.J. Morgan, J. Proudfoot

August 14, 1991

SDC-91-00052
ANL-HEP-TR-91-69

FIBER-TILE OPTICAL STUDIES AT ARGONNE

David G. Underwood
23 July 1991

In support of a fiber-tile calorimeter for SDC, we have done studies on a number of topics. The most basic problems were light output and uniformity of response. Using a small electron beam, we have studied fiber placement, tile preparation, wrapping and masking, fiber splicing, fiber routing, phototube response, and some degradation factors. We found two configurations which produced more light output than the others and reasonably uniform response. We have chosen one of these to go into production for the EM test module on the basis of fiber routing for ease of assembly of the calorimeter. We have also applied some of the tools we developed to CDF end plug tile uniformity, shower max testing and development for a couple of detectors, and development of better techniques for radiation damage studies.

I) Measurement Facility

In order to measure uniformity of response of layers in a sampling calorimeter, one would like to have a source of excitation which is as localized as an electron shower in the first few radiation lengths. One also needs to know the response to minimum ionizing particles. While some useful measurements can be made by measuring dc current output from excitation by UV lamp or radioactive source, there are a number of pitfalls that can be avoided by using a small penetrating beam of minimum ionizing particles.

We have built a tile mapping and measurement facility. It consists of a focussed electron beam, trigger scintillators, a two dimensional motor driven frame, electronics, and data acquisition and analysis programs (Fig. 1). This

facility was used to evaluate many different tile-fiber configurations. We have developed a 3 MeV electron beam by utilizing a Ru106 source and a spectrometer and focussing system of permanent magnets (Fig. 2). At this energy the electrons are approximately minimum ionizing in the first several mm of plastic scintillator. The range is great enough to penetrate a 5 mm thick tile, and a 2 mm thick trigger scintillator, and to give a signal in another thicker trigger scintillator. Multiple scattering in the first 2.5 mm of scintillator is not too serious for our spatial resolution of less than 2 mm. By using two trigger counters in coincidence we eliminate non-local and non-penetrating backgrounds such as gamma rays and low energy electrons. By focusing with quadrupoles and dipoles we get an adequate flux in a small spot size. Commercial sources of Ru106 of 1 milli-Curi have a diameter of about 5 mm. We have focussed this to 2 mm by 8 mm full width for all particles with a captured phase space of 200 mm-mr (Fig. 3). The rate is a few hundred hertz and we are limited in mapping speed by computer dead time.

The optical design for the spectrometer was done using the program "Transport" and checked to the extent possible with the Monte-Carlo program "Turtle". The spectrometer consists of two sections, an achromatic bending and focussing section, and a quadrupole doublet final focus section. This arrangement provides momentum selection as well as focussing and demagnification with limited chromatic aberrations. The first section utilizes two sector magnets of 45 deg. bend each, and a quadrupole between them to make the bend and focus achromatic. The magnets utilize ceramic (ferrite) material with a relatively low B-residual of 2.4 kG. The quadrupoles are made in sectors with no iron and have a gradient of 51. T/M. The worst one has about 5% octapole at the 5 mm radius. The sector magnets have iron flux returns and magnetic poles. The field is about 1.7 kG. Most of the beam transport is in vacuum to limit multiple scattering. The system is being patented by the U.S. Department of Energy.

We calibrate the number of photoelectrons per minimum ionizing particle by using a light-emitting-diode pulser with a fiber to the same photocathode as the fibers from the tile. Since the variation in pulse height due to variation in light output from the LED is small compared to the variation due to photostatistics, we find the number of photoelectrons at a given pulse height from the square of mean/sigma (Fig. 4). This method has been evaluated over a range from 0.6 to 10.2 photoelectrons by means of neutral density filters and has been found to be consistent. The pulse height depends on high voltage, phototube gain, etc. but the number of photoelectrons for a given setup is almost constant for each photocath-

ode. We have used a special LED pulser system developed at Argonne for CDF. By impedance matching, using absorbing resistors, etc. the complete pulse is less than 100 ns long and low voltages are used which do not damage the LED (Nucl. Instum. and Meth. A26, 351 (1988). .

TABLE 1

LED Pe Calibration Data

ND filters	Mean	Sigma	NPe	ADC counts/pe
0.3	706	219	10.2	69
0.7	268	133	4.0	67
0.7 + 0.3	106	82	1.67	63
0.7 + 0.7	38	49	0.60	63

II) Phototube Response

For a good tile-fiber unit we have the number of photo-electrons for four kinds of phototubes, and we plan to investigate more.

Table 2

Photocathode Efficiency
(all bi-alkalai), Green Light from BCF-91A Fiber

Tube	Stages	Typical N Photoelectrons
Amperex 2230	12	1.9
EMI 9839	12	3.0
Hammamatsu R580	10	3.4
Phillips 2081 Green Ext.	10	1.9
Phillips 2081 Green Ext.	10	2.9

We have only recently been able to investigate 10 stage tubes reliably due to the broadening effects of amplifier noise. A low noise amplifier with a gain of 100 is now used for 10 stage tubes and an amplifier with a gain of 10 for 12 stage tubes. This is for individual tiles with single minimum ionizing particles.

III) Scintillator Light Output

We have tried a number of combinations of tile and fiber:

Thickness	Configuration	Wrapping	Number Pe
2.5 mm	RH4, two straight fibers, mirrored ends	White Paper	1.0 to 1.1
2.5 mm	Styrene, 4 U fibers, bends outside	White Paper	1.65 to 2.0
5 mm	SCSN38, two straight fibers, mirrored ends	White Paper	1.7
2.5 mm	RH4, U fiber, 2.8 M clear spliced on	Aluminum Mylar	2.5
2.5 mm	RH4, U fiber, 2.8 M clear	White Paper	1.66
2.5 mm	RH4, U fiber, 2.8 M clear	Black Tedlar	0.9
2.5 mm	RH4, U fiber, 60 degree beveled edges,2.8 M alum. mylar	Aluminum Mylar	1.75
2.5 mm	RH4, 2 fibers with 4 ends to phototube,2.8M	Aluminum Mylar	2.0
2.5 mm	RH4, one loop fiber, 2.8 M clear	Aluminum Mylar	3.0

Some of these configurations are illustrated in Fig. 5.

We have also looked at relative outputs of some scintillator materials.

SCINT	SPLICE	CLEAR Fiber	GROOVE	MYLAR Side	COUNTS ADC	PE
RH1	ANL	2.8M	LSU	?	90	1.64
RH1	FNAL	2.5	LSU	?	98	1.78
RH4	ANL	2.8	LSU	?	119	2.16
Styrene	FNAL	2.5	FNAL-SP1	A	140	2.54
PVT	FNAL	2.5	FNAL-SPI	A	300	5.45
PVT	FNAL	2.5	FNAL-3D	B	240	4.36

The Bicron RH1 and RH4 were materials available in March 1991. Different versions have been developed recently. It was later determined that most of the difference between the PVT tiles was due to a bad fiber splice and that the side of the mylar used doesn't matter.

IV) Choosing a Buildable Configuration

We originally tested tiles with two straight waveshifter fibers with aluminized ends. These were abandoned due to poor light collection, poor uniformity, and inadequate reflectivity of the aluminization. The aluminized end of the fiber was rough when observed with a microscope. A Monte Carlo of the response pattern agreed reasonably well with the measured map (Fig. 6).

We next tried a U shape fiber pattern similar to that used by several other groups. The light output was better than with two cut fibers, but the map was not uniform. We found that in the case of a tile with polished edges, this could be rectified purely by fiber placement. Making the U into a wider loop at the bottom and narrow at the top in a dog bone shape produced a very flat response (Fig. 7).

We have recently concentrated on studies of the one-loop design with the fibers coming out the top surface of the tile. This is because of the calorimeter assembly problems with other designs which involve threading the 3-meter optical fibers through the calorimeter slots in the phi direction. Also the one-loop has the best light output and can be made to work with little or no masking (assuming our particular aluminized mylar wrap on face and edges). The EM cast lead prototype calorimeter has gaps of 4.5 mm between lead plates of 1 R.L. This gap accommodates the 1 mm fibers, the 2.5 mm tile, and steel splints and wrapping.

Our initial hope was to build this with no glue whatsoever because of the troubles encountered by CDF with glue on their fibers and because of the non-radiation hardness of some epoxies. We tried to use purely mechanical splints to reinforce the splice between waveshifter and clear fibers. We began studies of masking the reflected light from the aluminized mylar wrap in order to get uniform response. It was found that tiles of this design had a decaying light output with a 1/e time of 10 days.

After numerous tests of the time stability of the optical fibers, we found the problem occurred only in splices under mechanical stress. We tested the light transmission of Kuraray clear fiber, Bicron BCF-91a, and fibers made up of alternating segments of these spliced together. Eventually, two tiles were tested with steel hypodermic tubing glued over the splices for reinforcement (Fig. 8). These showed no decay over time during the rest of the month. The external routing is shown in Figs. 9 and 10.

V) Wrapping and Masking and Edge Preparation

We have studied both how the light output from a tile depends on the wrapping and how the wrapping can be modified, "masked" to control the response locally. One surprise in our studies was the extreme non-locality of response to black and highly reflective areas of the wrapping. This is illustrated in Figs. 11 (a) and (b). Our first approach to making the response uniform was to try using localized black non-reflecting areas on the reflective wrapping. This approach was successful for CDF central and Zeus wave shifter plates and also for the more closely related CDF plug upgrade prototype scintillation tiles. We soon realized that this was not a simple approach due to the non-local effects of masking. In our case the non local aspect was worsened because we could not use diffusive wrappings such as white paper but had to use extremely reflective wrapping to get enough light output. Given this constraint, it would be much better to control the response purely by the fiber placement if at all possible.

Another problem is that the uniformity of tile response depends on the length of the wave-shifter fiber leads outside the tile. If the light attenuation were simply exponential at one wavelength and the two leads were equal length, this would not be true. In the case of our loop configuration, the response would simply be slightly higher on the side of the tile near where the fibers exit. The observed dependence may involve cladding light vs. core light. In any event, we resorted to mapping only with the final external fiber configuration including splices and 2.5 meter clear fiber.

In our first attempt at masking, we found that two small black areas on one side only of the reflective wrap would produce most of the desired uniformity. It was difficult to control the placement of the mask and production was very labor intensive. We expected that the final masking design would depend on the final fiber splicing quality, the laser cutting on the edges of the tiles, and the 3-D geometry chosen for the groove where the fibers exit the tile and are routed on top of the tile between the plates of the calorimeter.

Recently we have tried simply covering the exiting fibers with aluminized mylar in the region of overlap so that double counting is avoided or decoupling is achieved. This appears to work very well and is much easier to build. In some maps there is a residual localized spike in the response (Fig. 12). This is because the covering of the fiber was not done where there is tape that holds the fibers

down during assembly. This problem could be avoided with advanced planning of the wrapping position before taping.

Another aspect of light level and uniformity is the edge preparation on the tile. Our early sample tiles were milled on the edge and then optically polished. This has little influence on the light collection inside the fiber loop, but affects the corners particularly. We have found that the 1 mm fiber cannot reliably be bent to smaller than a 2.5 cm radius, so there is significant area at the corners of the tile outside the fiber loop. One can show that with good optical edge preparation the corner light collection should be quite good. The solid angle to the fiber is available in one direction and a retro-reflector action utilizing both total internal reflection and aluminized mylar reflection is available in the other direction. In fact the response in the corners of the test tiles was very close to the tile center response. The laser cut tiles show significantly lower corner response. A comparison of laser cut vs. milled but not polished edges is shown in Figs. 13 and 14. The curving fall off is due to the larger vertical size of the electron beam so that some misses the tile in this corner-to-corner diagonal scan. The corner response is acceptable in tiles which have milled edges without optical polishing, and better than for laser cut tiles. This still assumes that aluminized mylar is flat against the 2.5 mm high edge.

Another issue is tile to tile uniformity. In our tests so far this looks adequate. We will need more tests with various sizes of tiles. A crude example of what can be done is shown in Fig. 15.

An issue which may arise, in a particular calorimeter design, is sloping of the edges of tiles to accommodate mechanical supports between projective towers. We tested this with an early fiber design and found that the only problem was somewhat reduced light output. This is noted in Fig. 5.

VI) Tile Preparation

The actual tiles for the EM test beam module were cut at Laser Services in Massachusetts from RH4 material supplied by Bicron. The cutting service had to experiment extensively in order to cut this new material with an optical surface at right angle to the larger tile dimensions. They had previously been very successful with SCSN81 scintillator for the ZEUS calorimeter. They also had to anneal our material at a lower temperature, 125° F, to prevent eventual crazing. The tiles have a small ridge at the corner between edge and flat surface from the laser

cutting. A few of the tiles have some surface damage due to splattered molten plastic from the cutting process. They are coated with an emulsion, "Emulsitone" before cutting to minimize scratches during handling. It is time consuming to wash off this emulsion by hand before grooves can be cut in the tiles. We do not want soap or emulsion to accumulate in the grooves. The transverse dimensions are 0.0 to 0.5 mm smaller than nominal, which is good for inserting tiles into the casting.

The material supplied was measured and weighed at Argonne and found to have average thickness of 2.61 mm and rms deviation of 3.6 %. Only enough scintillator material was available at this time for 6 towers of the 10 towers of the test calorimeter. Half the tiles were sent to LSU for grooving and half to Fermilab. They were selected on the basis of tile weight which correlates well with thickness. A table of tile weight vs. thickness was delivered.

VII) Fiber Preparation and Testing

About 10 % of the fibers for the EM test beam module were spliced, splinted, and polished at Fermilab on June 26-27. The one fiber tested at that time in an actual tile gave 13% more light than our test fibers spliced at Argonne. (The Argonne splicer supplied by Rockefeller had a broken quartz tube and only an oversize replacement was available immediately.) The remaining fibers were done in small batches and complete by July 19, except for replacements. Typical Rockefeller splicer results are shown in Fig. 16.

A fiber assembly testing box has been built. It reads the 8 ends of 4 fiber assemblies simultaneously, for immediate spotting of problems. Further data analysis is done on the data collected to look for more subtle problems. PIN diodes are used with current-to-voltage amplifiers and a 12 bit 8 channel adc in a PC computer. A length of wls fiber roughly equal to the length to be in the tile is illuminated by UV light. The box was originally tested with one fiber and performed as expected except that the clamps for the fibers were too difficult to use for mass-production testing. New clamps were designed and built. A sample of 124 fiber assemblies has been tested so far. Figure 17 shows the scatter in the raw fiber measurements. The decay of the light output from the UV lamps can be seen for the early measurements before we learned to warm up the lamp overnight. Also, the first batch of 32 fibers, (10 sets in the graph) show much more scatter than later sets. After cuts, we accept 90% of the fibers so far. The

acceptance is greater for later sets. After cuts and corrections for UV lamp variation we get about 3.9% rms variation (Fig. 18). Some of this comes from the variation in attenuation because the fibers for different size tiles are different lengths. The fibers used so far are 51 to 59 cm long and the attenuation length is about 130 cm. This gives a maximum difference of 6%. Some of the variation comes from the coupling to the PIN diodes. We have shown that if the fibers are not cut exactly at right angles there is a dependence on the rotation angle of the fiber when it is inserted in to the PIN diode holder. The PIN diodes have small (1 mm sq.) surface area and lenses which may be curved and off center.

CONCLUSIONS

We have developed a number of measurement tools for tile-fiber development. We have tested many configurations and have high-quality diagnostic information on them. We have evolved a design which is buildable for an SDC electromagnetic calorimeter prototype without compromising the physics. Our techniques also allow higher quality measurements which are useful for other detector development work such as for shower max detectors and radiation damage studies.

ACKNOWLEDGEMENTS

We acknowledge a mutually beneficial interaction with the CDF plug upgrade prototype group. We have worked particularly closely with Pawel de Barbaro and Brian Weiner. We thank Sebastian White, of Rockefeller, Karen Kephart and Sui Lu, of Beijing, for help splicing fibers. At Argonne we have had help from Norm Hill and Joe Sheppard in building apparatus. Most of our tile machining was supervised by Ali Fazely, of Louisiana State University, and some prototypes were done by Jon Blomquist of Fermilab. We thank Tom Kirk, Larry Nodulman, and many SDC collaborators for helpful discussions, and Ruth Hill for help with the manuscript.

* *Work supported by the U.S. Department of Energy, Division of High Energy Physics, Contract W-31-109-ENG-38.*

FIGURE CAPTIONS

Figure 1 — The tile-fiber test system. In addition to the electron beam there is light injection to the photocathode for calibration. A 286-based computer is used for x-z mapper control and Camac data acquisition.

Figure 2 — Ru106 Source Beamline layout. The quadrupoles and dipoles utilize permanent ceramic magnets. The electrons are momentum selected to 3 MeV/c ± about 5%. The source of 5 mm dia. is demagnified to give a spot 2 mm × 7 mm for all particles after chromatic aberrations, etc.

Figure 3 — Width of the beam spot containing all electrons detected with polaroid film. A fit to the beam envelope gives ex = 200 mm-mr and B*x = 5 mm.

Figure 4 — A typical pulse height spectrum from the LED. The number of photoelectrons is determined from $(\text{mean/sigma})^2$ and the number of ADC counts/photoelectron is determined. The results are consistent when the amount of light is changed over an order of magnitude by means of neutral density filters.

Figure 5 — Light output from some tile-fiber configurations.

Figure 6 — Monte-Carlo tile response map. The program was written at Purdue and set up and run for this configuration at Argonne. The enhanced response with a dip at the fiber is typically observed in real tile maps.

Figure 7 — Example of a tile-fiber map for a configuration which has good uniformity with no mask but which requires fibers to be threaded through the calorimeter. We have chosen a different configuration which is simplifies calorimeter assembly.

Figure 8 — Fiber pattern chosen for our prototype. The loop of fiber in the tile can be seen as well as the external fiber routing and the steel reinforcements on the splices.

Figure 9 — A drawing of the fiber routing on the face of the calorimeter.

Figure 10 — A model of one tower showing fiber routing.

Figure 11 a,b Masking studies showing non-local effects. a) Response map from a tile with black tedlar wrap and aluminized band around the tile. b) Response map form a tile with aluminized mylar wrap and a black band around the tile.

Figure 12 Response MAPS from a laser cut tile with our chosen fiber routing. The corner response falls off for laser cut tiles. There are peaks due to scintillation of WLS fiber and incomplete wrapping for decouping at the overlap.

Figure 13 Response map (corner to corner) of a tile of our chosen design with machined but unpolished edges. The response in the corners is better than for the laser cut tile.

Figure 14 Response map (corner to corner) of a tile of our chosen design with laser cut optically clear edges. The response outside the fiber loop is low, presumably due to waviness of the edge and reliance on a combination of total internal reflection and reflection from aluminized mylar.

Figure 15 Tile to tile uniformity. These tiles were from the CDF end plug prototype. The notch between them goes away when the tiles are closer to each other.

Figure 16 Rockefeller fiber splicer results. They obtained 10% ± 2% light loss in this test.

Figure 17 Light output from 248 mass-produced fiber sets before culling the ones with weak response. Variation of the UV lamp used to excite the fiber has not been removed from this plot.

Figure 18 Light output from the fibers accepted for the prototype module. 90% of the fibers were acceptable at this stage. The RMS variation is 3.8 %.

TILE-FIBER TEST SYSTEM

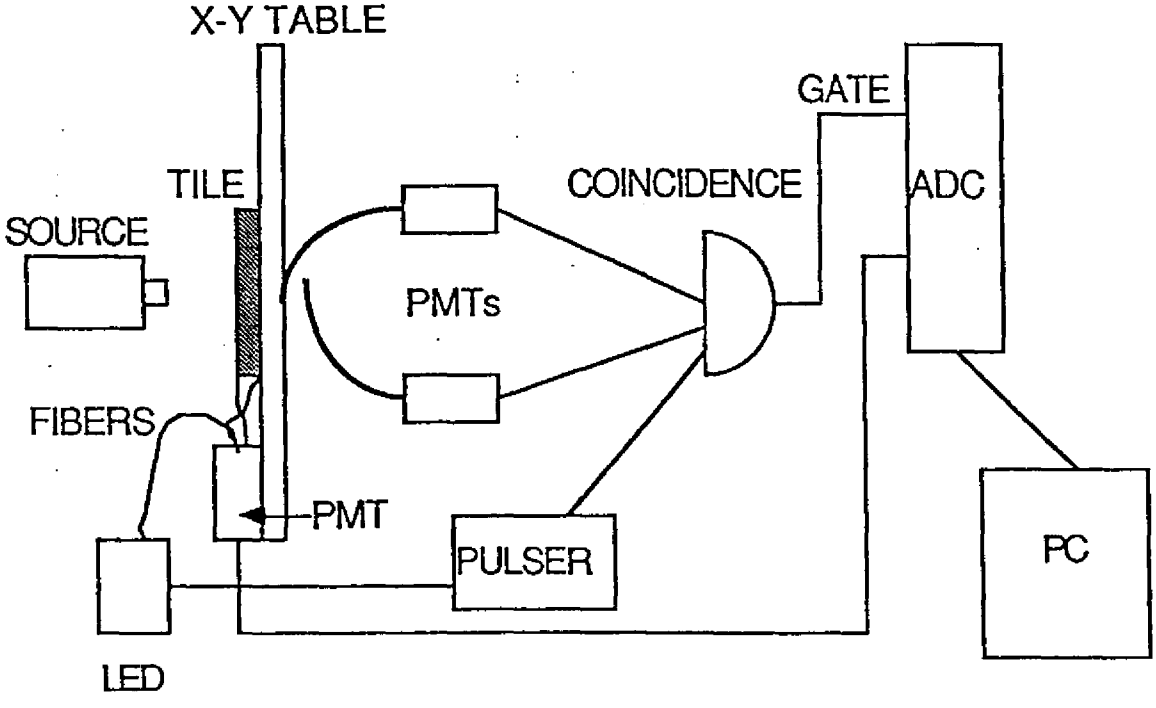

Figure 1

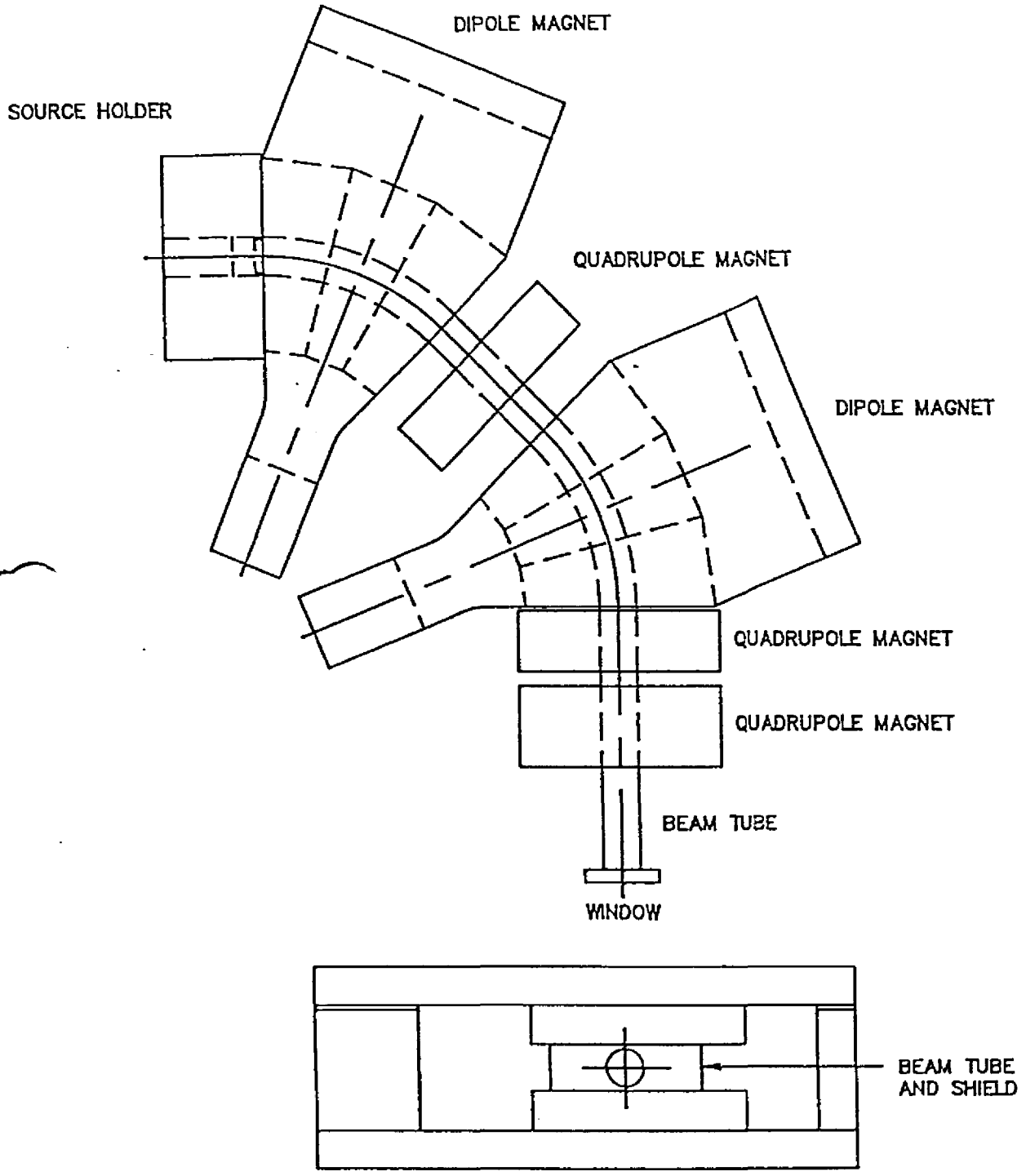
DIPOLE MAGNET
SOURCE HOLDER
QUADRUPOLE MAGNET
DIPOLE MAGNET
QUADRUPOLE MAGNET
QUADRUPOLE MAGNET
BEAM TUBE
WINDOW
BEAM TUBE
AND SHIELD

Figure 2

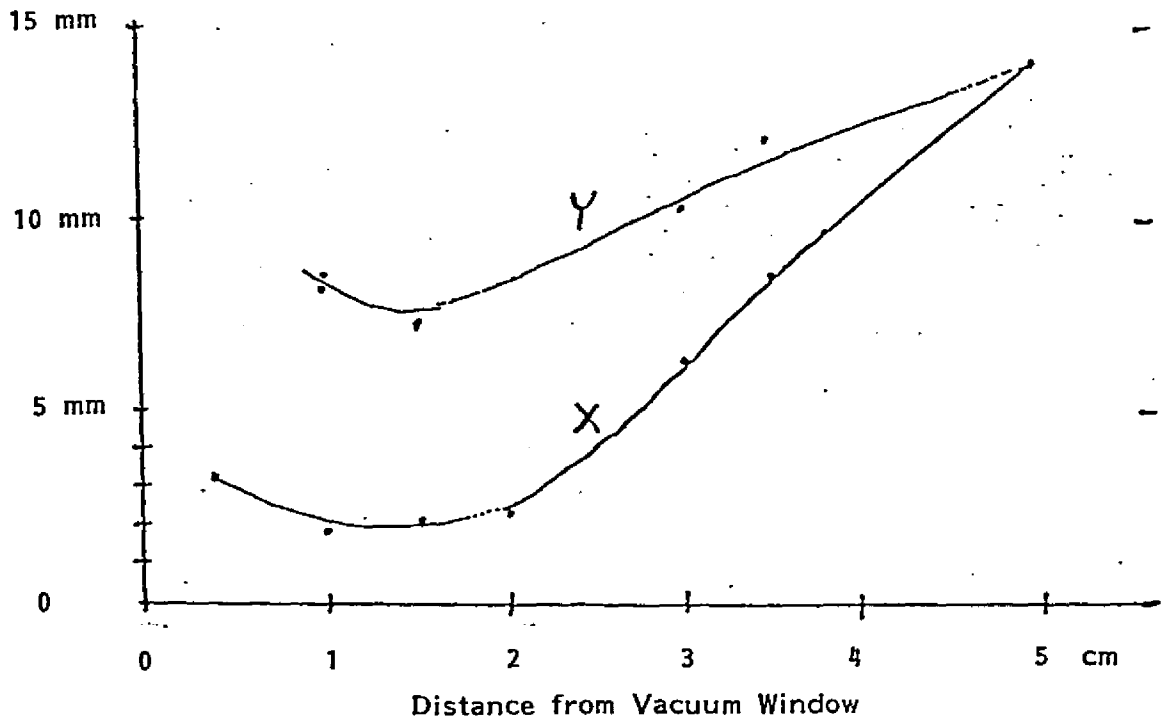

Width of the beam spot containing all electrons detected with polaroid film. A fit to the beam envelope gives ε_x = 200 MM-MR and β^*_x = 5 mm.

Figure 3

LED WIDTH CALIBRATION CONSISTENT 0.6 -10 pe

7.3 pe => $\sigma/m = 0.323$

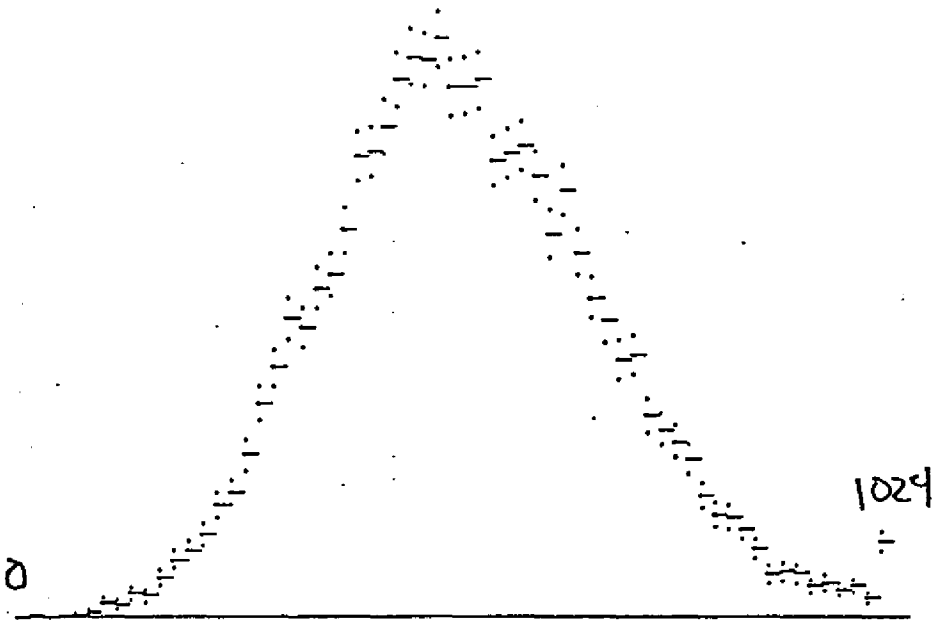

Figure 4

LIGHT YIELD AT CENTER NO MASKING

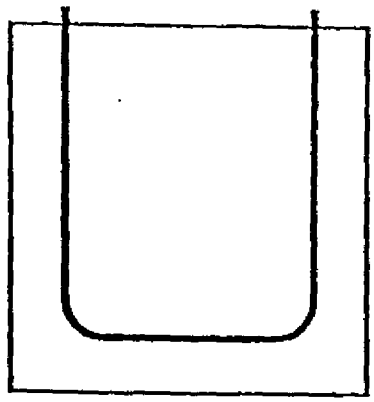

RECTANGULAR EDGE

WRAP:	pe/mip
BLACK TEDLAR	0.9
WHITE PAPER	1.66
AL. MYLAR	2.47

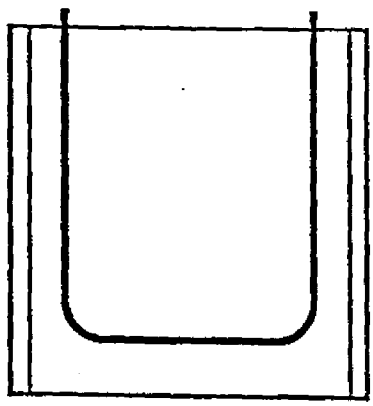

ANGLE CUT EDGE

AL. MYLAR 1.75

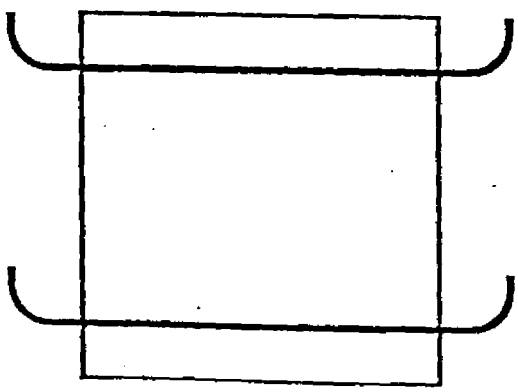

AL. MYLAR 2.0

ALL DATA FOR
2.8 M OF CLEAR
FIBER

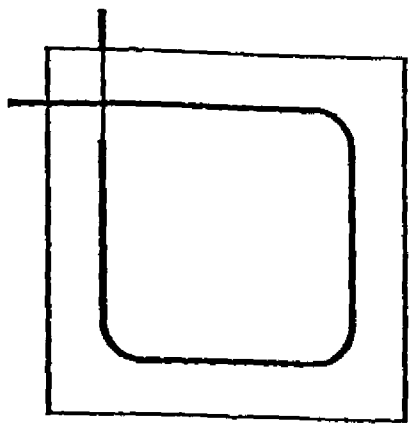

AL. MYLAR 3.0 pe/mip

Figure 5

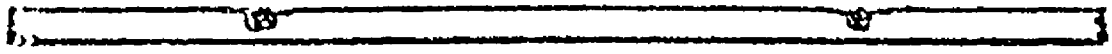

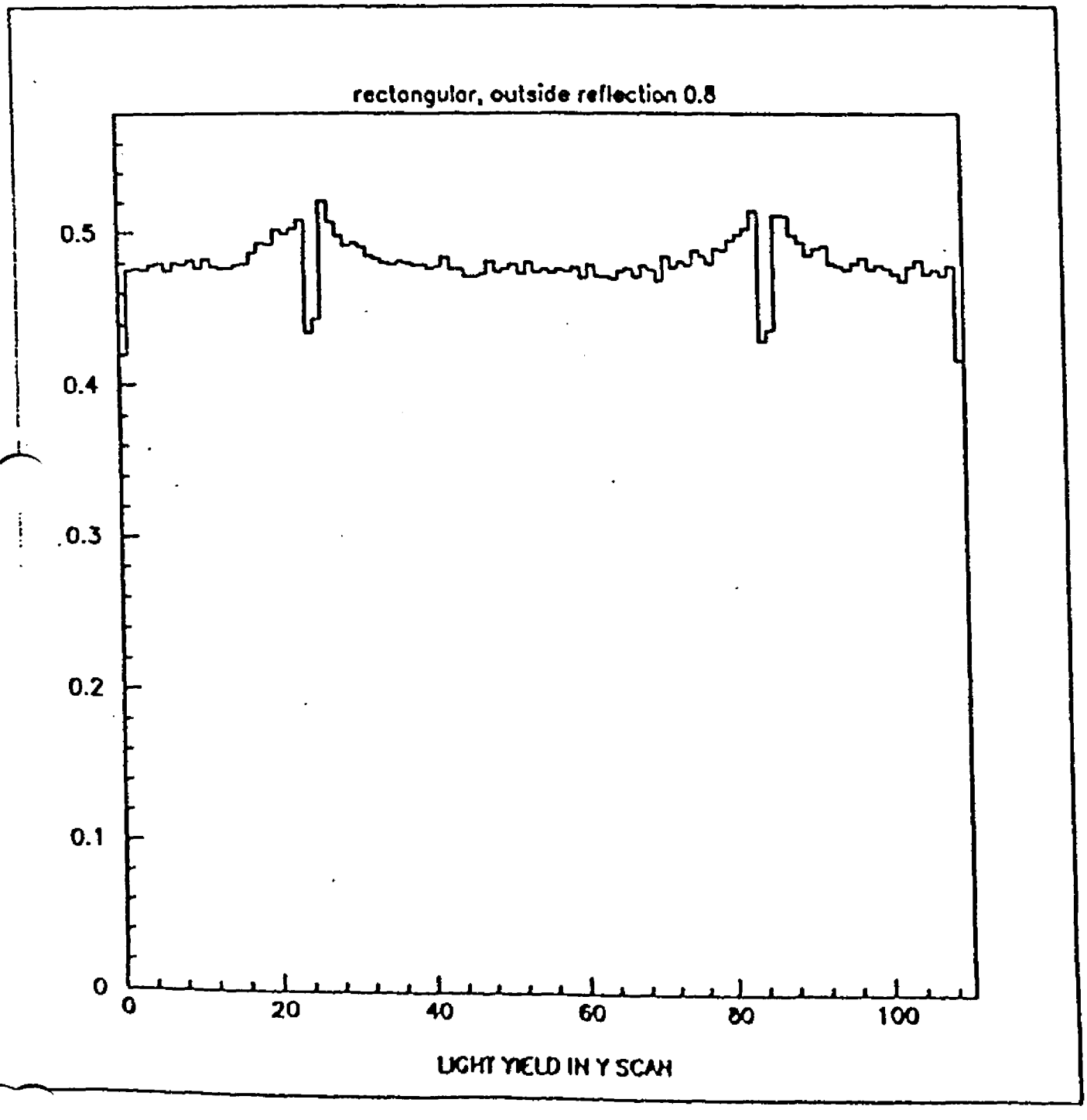
rectangular, outside reflection 0.8
0.5
0.4
0.3
0.2
0.1
0
0
20
40
60
80
100
LIGHT YIELD IN Y SCAN

Figure 6

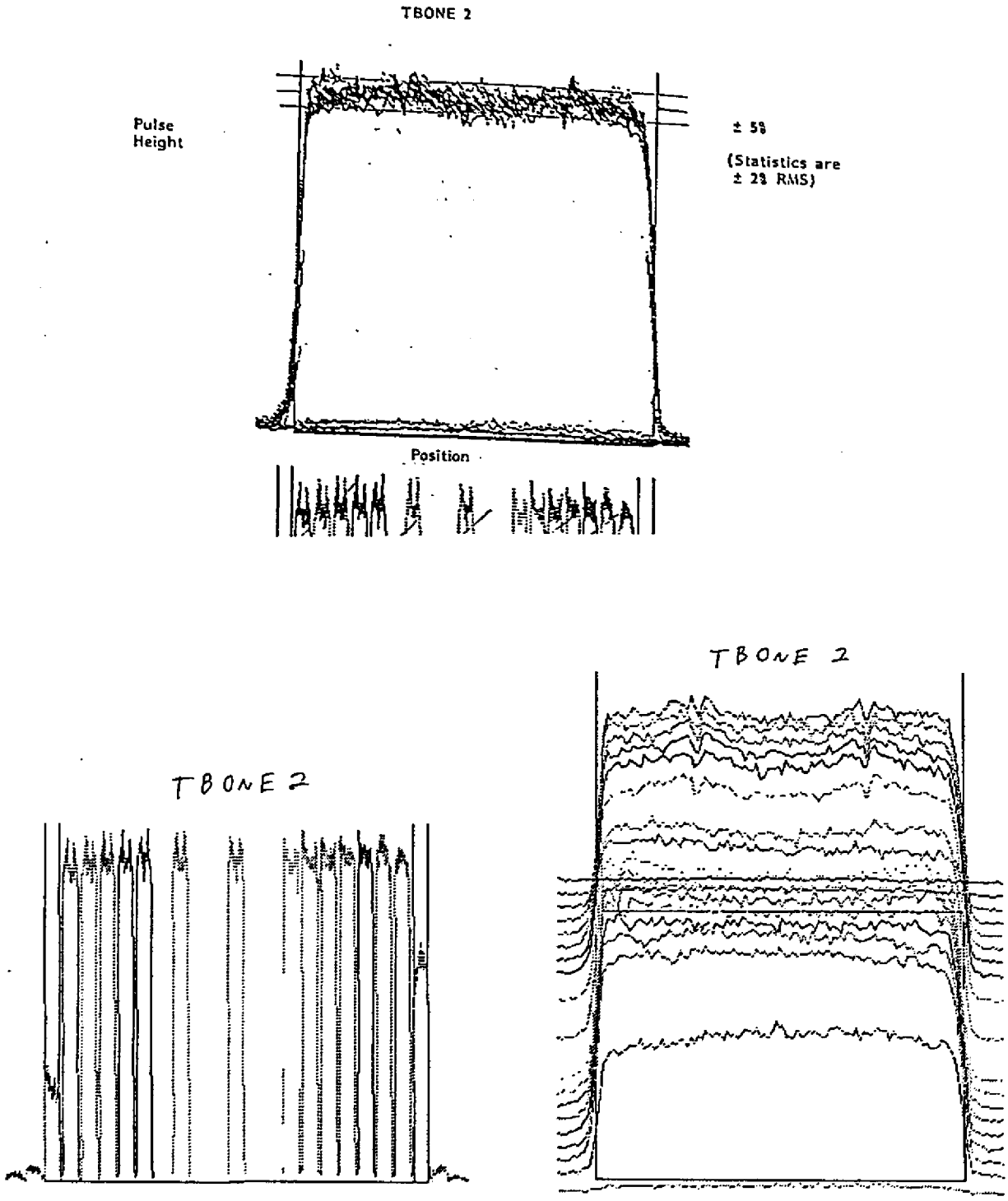
TBONE 2
Pulse Height
± 5%
(Statistics are ± 2% RMS)
Position
TBONE 2
TBONE 2

Figure 7

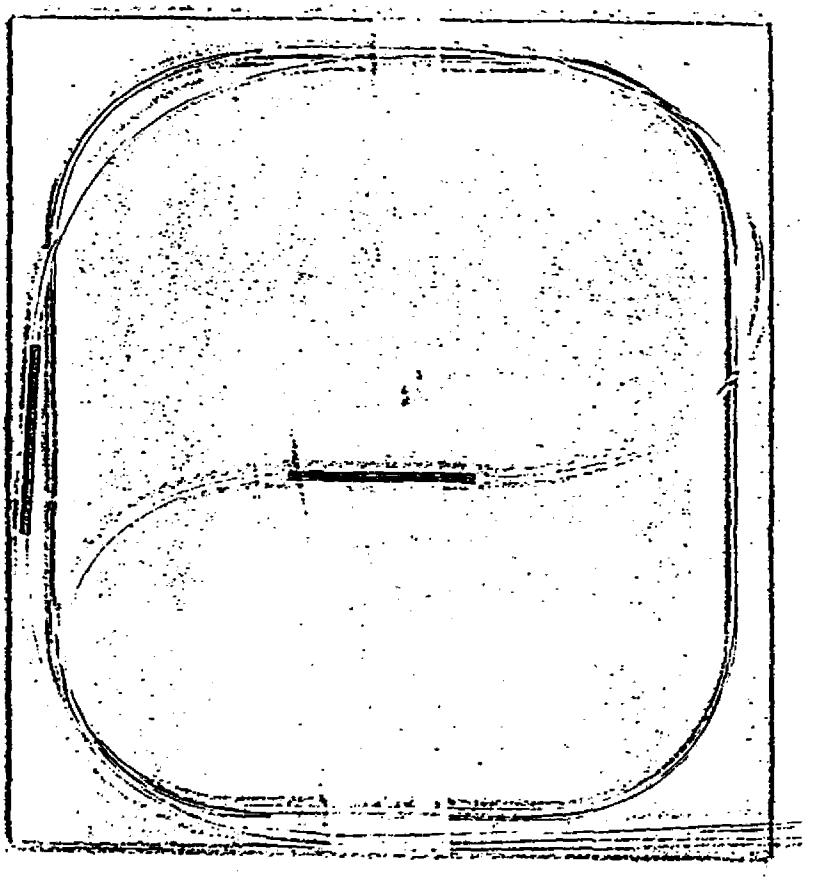

A tile from EM Tower 2, Layer 29. The loop fiber path in the tile is shown as well as the external fiber routing. The steel ferrules are used to reinforce the splices between wave shifter fiber and clear fiber.

Figure 8

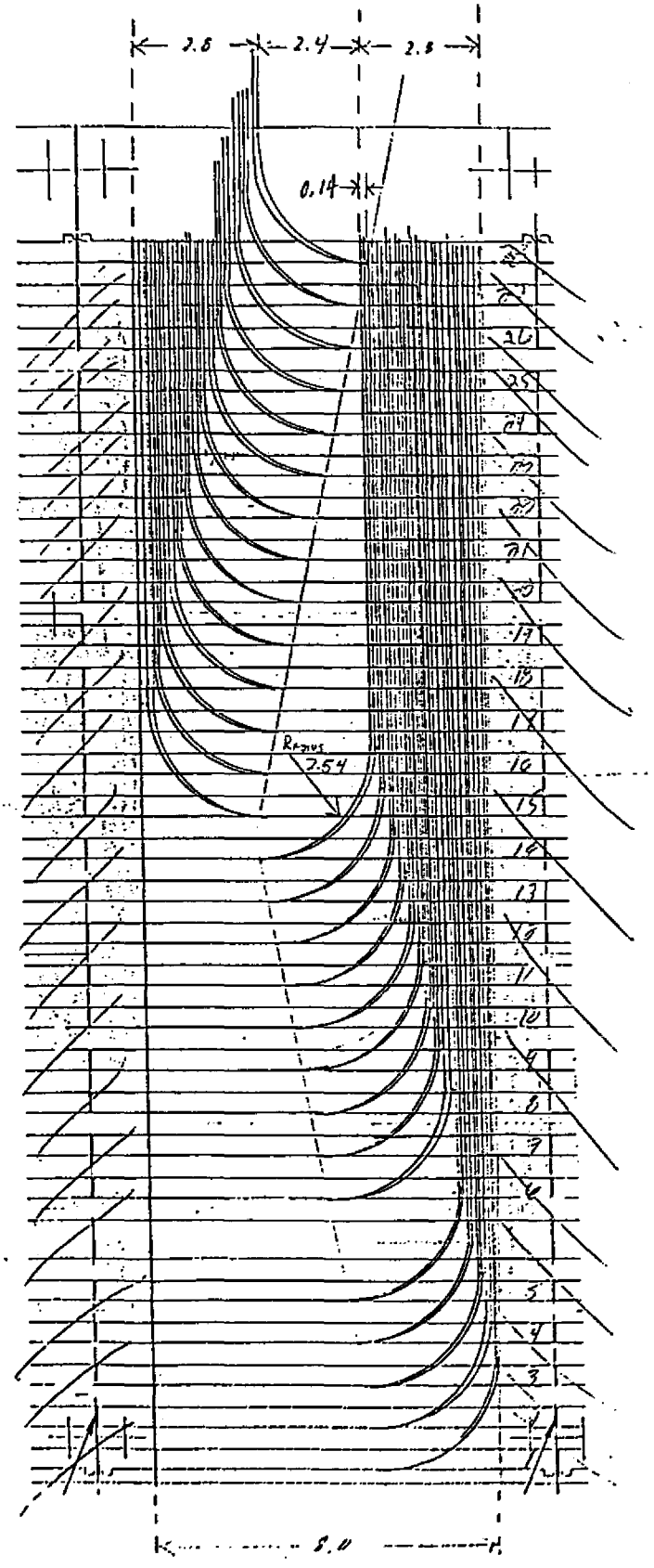

Figure 9

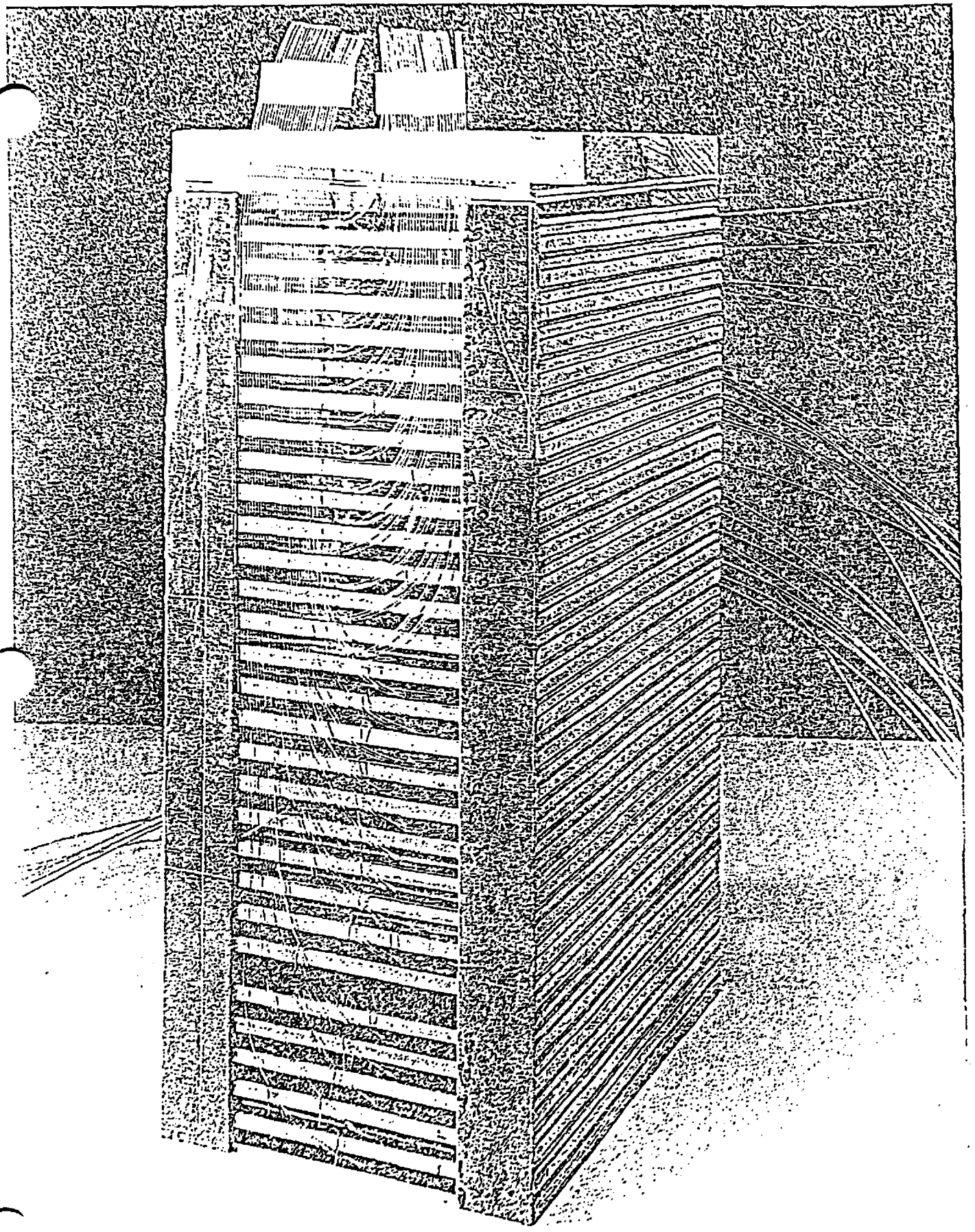

Figure 10

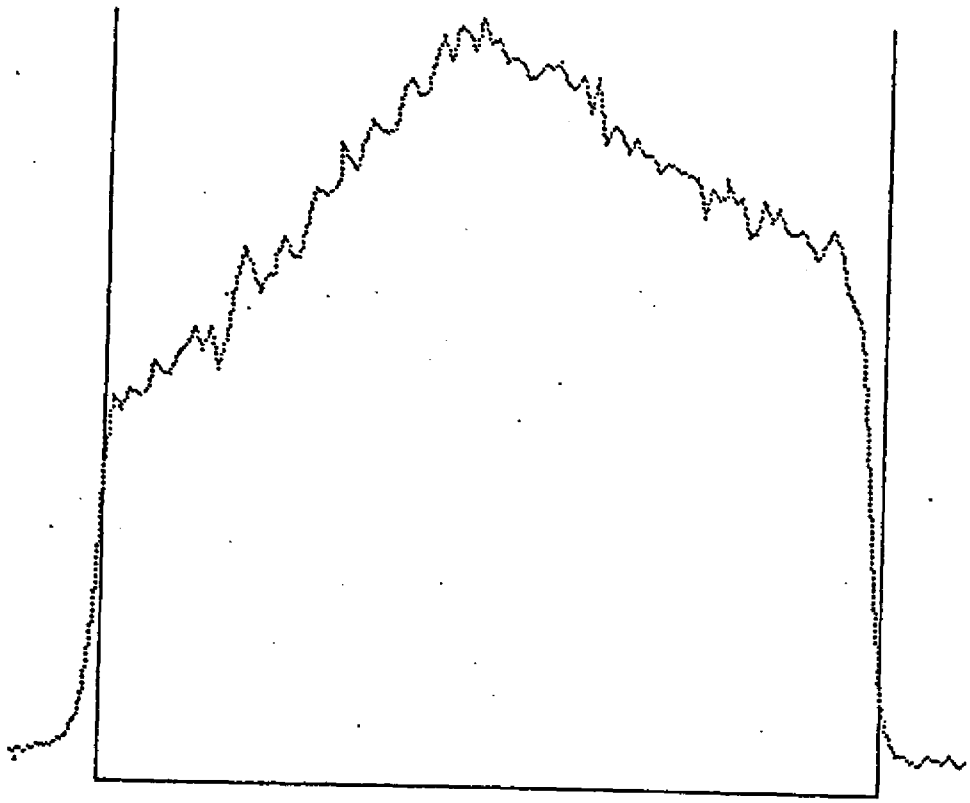

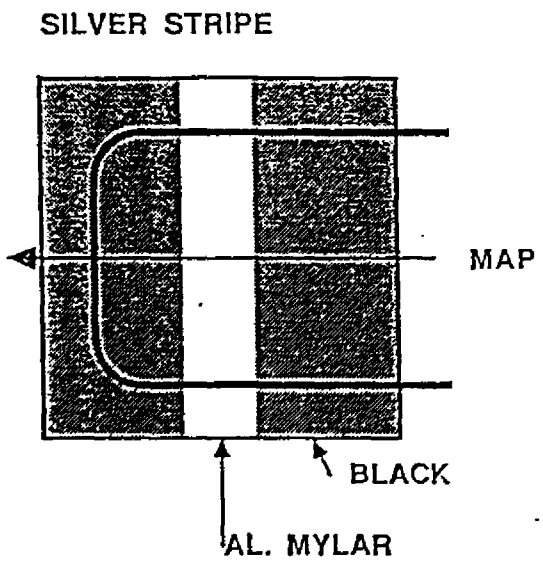

Figure 11 (a)

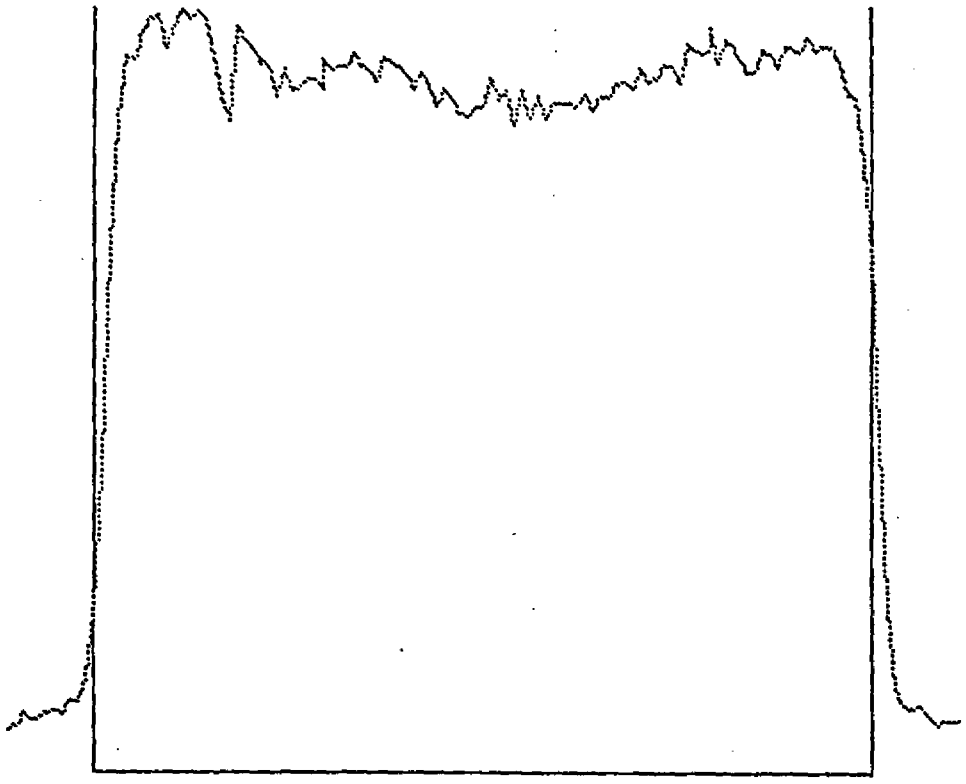

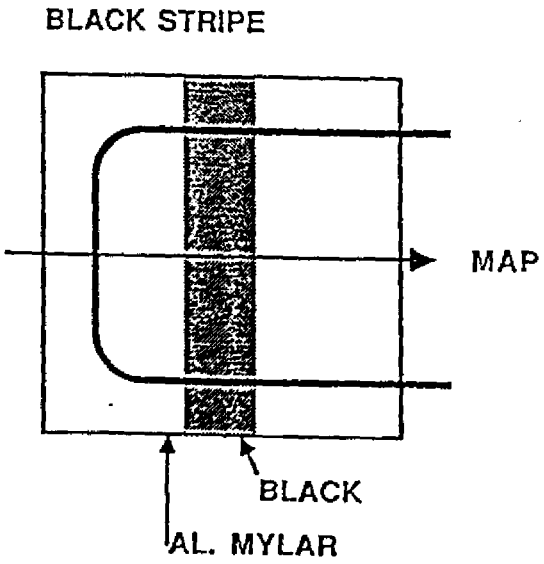

Figure 11 (b)

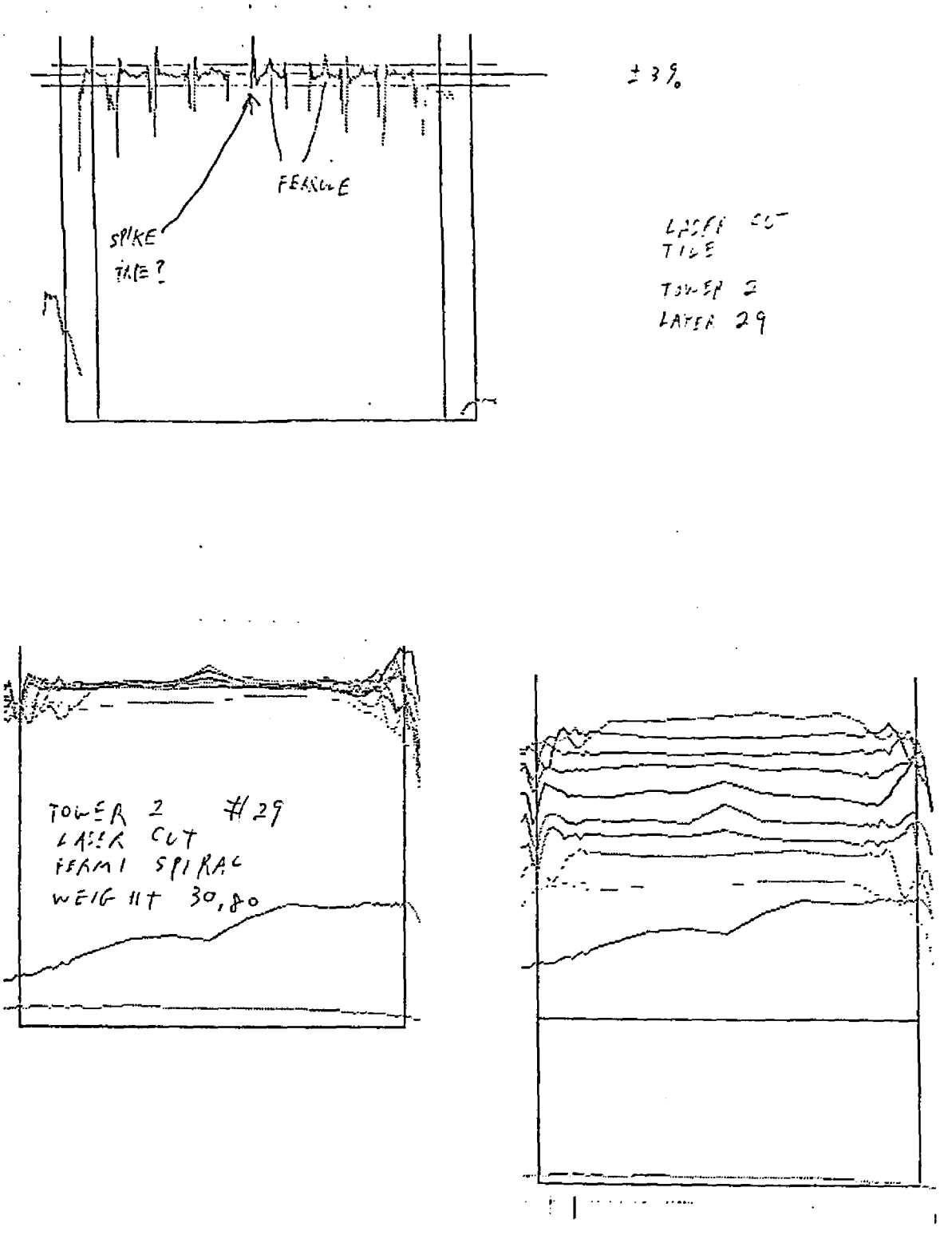
±3%
FERRULE
SPIKE
TIME?
LASER CUT
TILE
TOWER 2
LAYER 29
TOWER 2 #29
LASER CUT
FERMI SPIRAL
WEIGHT 30,80

Figure 12

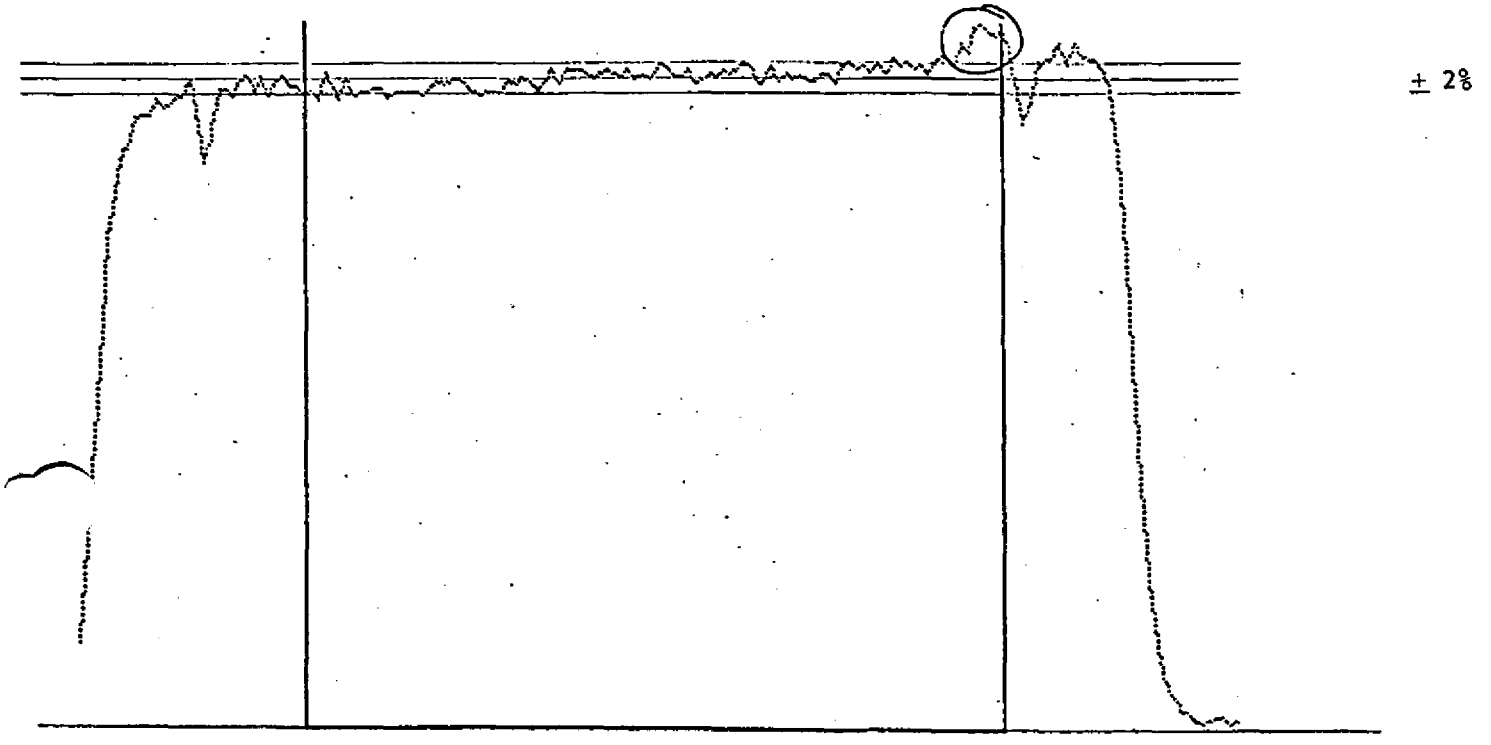

TPVTD1A 2

Figure 13

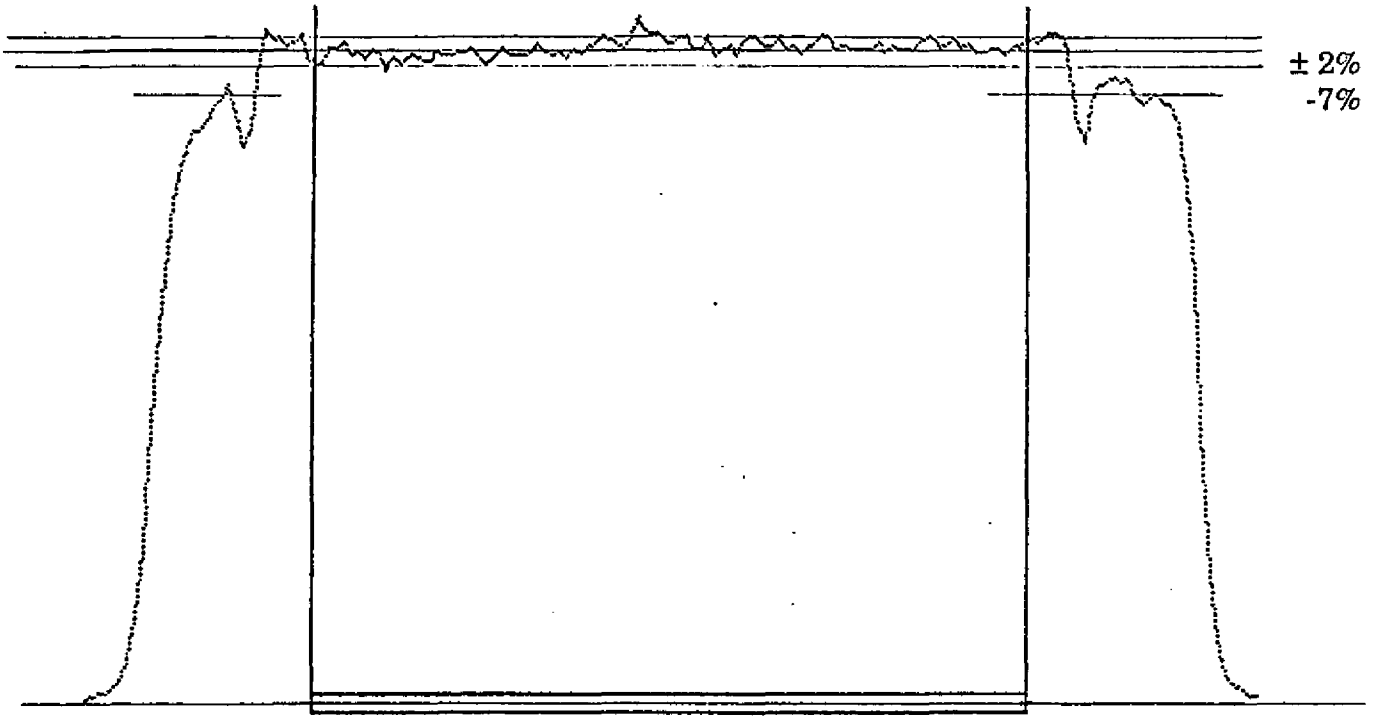

Laser Cut

T229BD1

Figure 14

TE 231310

MASKED

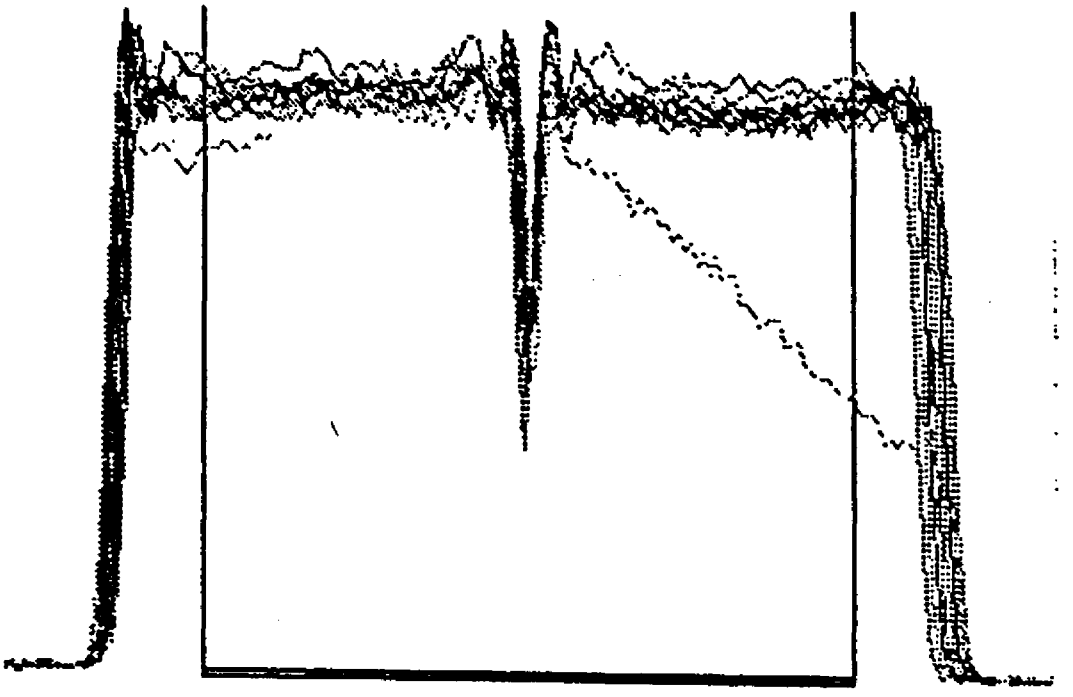

TILE TO TILE UNIFORMITY
(TILES WERE NOT CLOSE ENOUGH)

CDF END PLUG E.M.

Figure 15

SPLICING FIBER TEST USING CLEAR TO CLEAR

ROCKEFELLER SPLICER

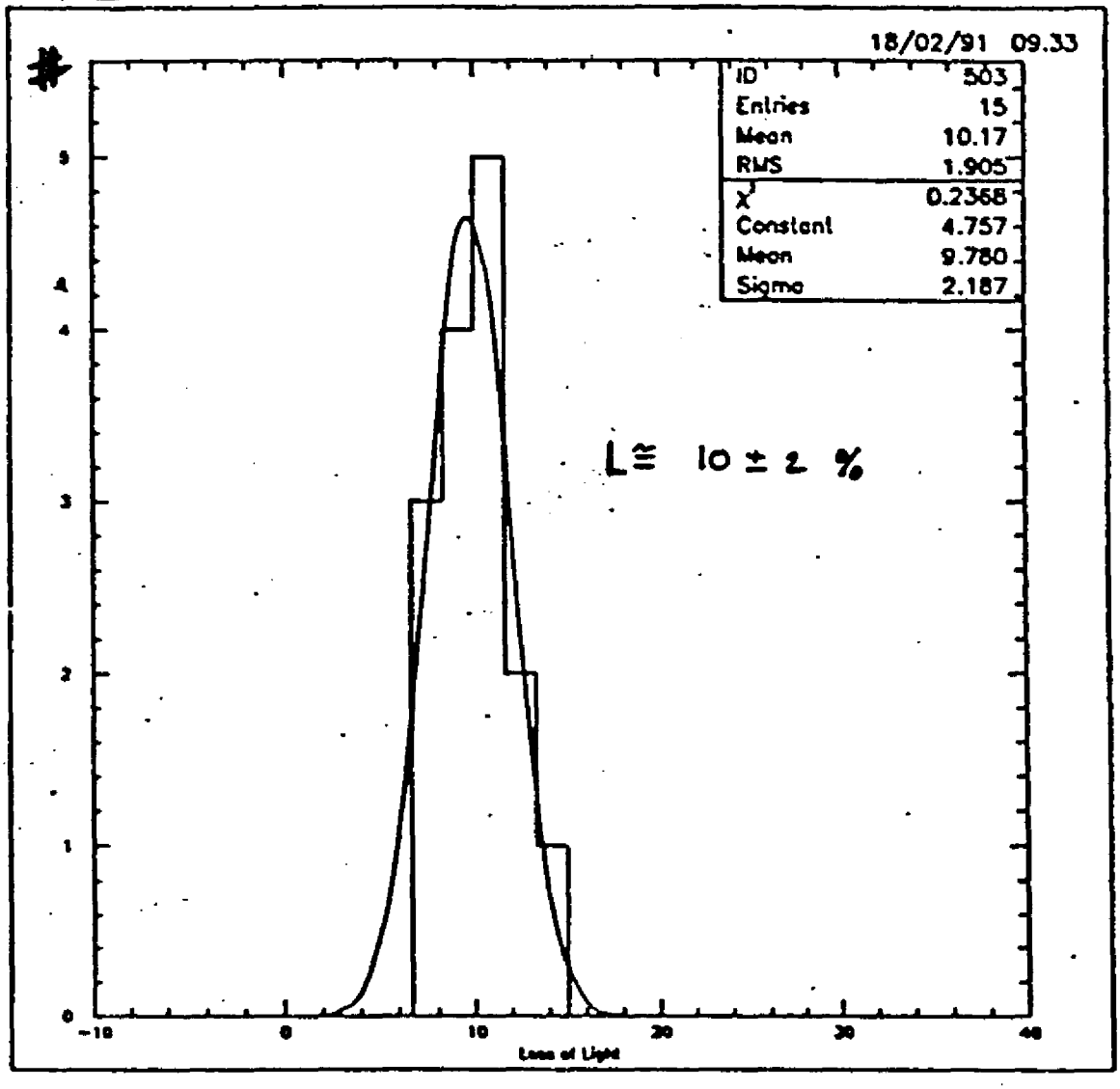

Loss of Ligh in %

Figure 16

del/MEAN VS SET

```
          ****************************
          *                          *
   39     *                          *
   38     *                          *
   37     *                          *
   36     *                          *
   35     *            223 +         *
   34     * +          +32   +       *
   33     *           2 222          *
   32     *           ++++2++        *
   31     *          ++ 42           *
   30     *            ++5 +         *
   29     *           +222 +         *
   28     *        + 2  ++2+         *
   27     *         ++ 3 2+          *
   26     *      +    +2+2 +         *
   25     *            ++23 +        *
   24     *                          *
   23     * +           3++ +     +  *
   22     *        +     222+        *
   21     * +          ++++3         *
   20     *      + +    2+3          *
   19     *        ++ 3+2            *
   18     *        +   33+           *
   17     *          +  + 5 +        *
          *           ++2 22         *
          *         +++++ 2+         *
   14     *              4+ 3        *
   13     *             +32 2        *
   12     *                          *
   11     *      +      2  2 2  +    *
   10     *                          *
    9     * +         +2+ +++        *
    8     *    + +   2++   + +       *
    7     *              2++3  +     *
    6     * +           +2   + ++  + *
    5     *                + +32+    *
    4     * +               2+3+     *
    3     *                          *
    2     * +       + ++  ++ ++      *
    1     *                 ++3 2 +  *
          *                          *
          *                          *
          ****************************
          1.             1111111111
          0   8888899999000001111 1
          0   0246802468024680246 8
```

Figure 17

del/M-TIME S cut

```
34
33                                  -
32                                  I
31                                  I
30                                  I
29                                  I
28                                  I
27                                 -I
26                                 II
25                              - II
24                              I II
23                              I II
22                              I II
21                              I II
20                              I II -
19                              I II I
18                              I II I
17                              I II-I
16                              I I  I
15                              I I  I
14                              I I  I -
13                              I I  I I
12                          -   I I  I I
11                          I  -I-I  I-I
10                          I  I       I
 9                          I  I       I
 8                          I -I       I
 7                         -I-I        I-
 6                         I            I
 5                         I            I
 4                         I            I -
 3                         I            I-I
 2                        -I              I-
 1                       -I                I-

     1.                            1111111111111111111111111
     0   7777788888888889999999990000000000111111111122222
     0   5678901234567890123456789012345678901234567890123
```

Figure 18